Scale-dependent interactions between tree canopy cover and impervious surfaces reduce daytime urban heat during summer

Carly D. Ziter[a,1,2], Eric J. Pedersen[b], Christopher J. Kucharik[c,d], and Monica G. Turner[a,1]

[a]Department of Integrative Biology, University of Wisconsin-Madison, Madison, WI 53706; [b]Department of Biology, Memorial University of Newfoundland, St. John's, NL A1B 3X9, Canada; [c]Department of Agronomy, University of Wisconsin, Madison, WI 53706; and [d]Nelson Institute for Environmental Studies, University of Wisconsin, Madison, WI 53706

Contributed by Monica G. Turner, February 19, 2019 (sent for review October 22, 2018; reviewed by Mary L. Cadenasso and G. Darrel Jenerette)

As cities warm and the need for climate adaptation strategies increases, a more detailed understanding of the cooling effects of land cover across a continuum of spatial scales will be necessary to guide management decisions. We asked how tree canopy cover and impervious surface cover interact to influence daytime and nighttime summer air temperature, and how effects vary with the spatial scale at which land-cover data are analyzed (10-, 30-, 60-, and 90-m radii). A bicycle-mounted measurement system was used to sample air temperature every 5 m along 10 transects (~7 km length, sampled 3–12 times each) spanning a range of impervious and tree canopy cover (0–100%, each) in a midsized city in the Upper Midwest United States. Variability in daytime air temperature within the urban landscape averaged 3.5 °C (range, 1.1–5.7 °C). Temperature decreased nonlinearly with increasing canopy cover, with the greatest cooling when canopy cover exceeded 40%. The magnitude of daytime cooling also increased with spatial scale and was greatest at the size of a typical city block (60–90 m). Daytime air temperature increased linearly with increasing impervious cover, but the magnitude of warming was less than the cooling associated with increased canopy cover. Variation in nighttime air temperature averaged 2.1 °C (range, 1.2–3.0 °C), and temperature increased with impervious surface. Effects of canopy were limited at night; thus, reduction of impervious surfaces remains critical for reducing nighttime urban heat. Results suggest strategies for managing urban land-cover patterns to enhance resilience of cities to climate warming.

urban heat island | urban forest | air temperature | ecosystem services | landscape context

The urban heat island effect (UHI), in which temperatures are higher in urban compared with surrounding rural environments (1, 2), presents a major sustainability challenge for cities. Owing mainly to replacement of vegetation with impervious surfaces, high city temperatures increase the vulnerability of urban residents to heat waves and climate warming and drive urban energy demands and costs upward globally (3–6). Extreme high temperatures are increasingly reported in cities worldwide, with record-setting heat reported in many northern hemisphere cities in summer 2018 (7). Strategies to improve cities' resilience to future climates are critical as urban areas expand, urban populations grow, and extreme heat events increase in frequency in a warming world (8, 9).

Although the broad-scale causes, magnitude, and spatial extent of urban–rural temperature differences have been studied extensively (2, 4), less is known about how landscape heterogeneity within cities affects local variation in temperature. Research linking land-cover patterns and land surface temperature (e.g., from satellite imagery) shows that the UHI is more an "archipelago" than an "island," with temperature differences between localized hot and cool spots as large as temperature differences along the urban–rural gradient (6, 10). However, spatially distributed measurements of local air temperature, a key metric for public health outcomes (11), at within-city scales relevant to adaptation (e.g., 10s to 100s of meters) are limited.

Studies of intraurban air temperature have focused largely on either impervious surfaces, which absorb and retain heat (1), or the "park cool island" effect, in which green spaces such as parks are cooler than built-up areas. Temperature within parks is further modified by the size, shape, and type of vegetated patches (12, 13). However, cities are not neatly divided into green and impervious spaces. Rather, natural and built features are integrated at fine scales within cities (14, 15), and features can even co-occur (e.g., tree canopy over pavement). Studies that quantify effects of land cover on urban air temperature across the range of spatial scales that incorporate this heterogeneity can provide a strong foundation for developing urban climate adaptation strategies. In addition, such studies must explore potential interactions between impervious cover and vegetation structure because they are not necessarily mutually exclusive at fine scales.

Urban trees may offer an important opportunity to mitigate high temperatures at the scale of urban residents' daily lives. Trees are prevalent throughout many cities, and unlike the relatively static size and shape of parks, the urban canopy continually changes. Canopy cover changes as trees mature and in response to policy, societal preference, disturbance, and pests or disease (16–18). The potential of trees to regulate temperature is widely acknowledged, with forested green spaces reaching much cooler temperatures than their nontreed counterparts (12, 13, 19). However, many

Significance

Cities worldwide are experiencing record-breaking summer air temperatures, with serious consequences for people. Increased tree cover is suggested as a climate adaptation strategy, but the amount of tree canopy cover needed to counteract higher temperatures associated with impervious surface cover is not known. We used a bicycle-mounted measurement system to quantify the interaction of canopy cover and impervious surface cover on urban air temperature. Daytime air temperature was substantially reduced with greater canopy cover (≥40%) at the scale of a typical city block (60–90 m), especially on the hottest days. However, reducing impervious surfaces remained important for lowering nighttime temperatures. Results can guide strategies for increasing tree cover to mitigate daytime urban heat and improve residents' well-being.

Author contributions: C.D.Z., C.J.K., and M.G.T. designed research; C.D.Z. and E.J.P. performed research; C.D.Z. and E.J.P. analyzed data; and C.D.Z., E.J.P., C.J.K., and M.G.T. wrote the paper.

Reviewers: M.L.C., University of California, Davis; and G.D.J., University of California, Riverside.

The authors declare no conflict of interest.

Data deposition: All data and scripts associated with the manuscript have been archived with the Environmental Data Initiative and can be found at https://portal.edirepository.org/nis/mapbrowse?packageid=edi.314.2.

[1]To whom correspondence may be addressed. Email: carly.ziter@concordia.ca or turnermg@wisc.edu.

[2]Present address: Department of Biology, Concordia University, Montreal, QC H4B2A7, Canada.

This article contains supporting information online at www.pnas.org/lookup/suppl/doi:10.1073/pnas.1817561116/-/DCSupplemental.

Published online March 25, 2019.

landscape-scale studies group trees alongside other vegetation (e.g., normalized difference vegetation index; other "greenness" metrics) despite the potentially greater cooling offered by trees compared with lower-stature vegetation (20). Trees and impervious surfaces can also have similar coverage at the same location, such as when roads, sidewalks, and roofs are covered by a closed canopy. Understanding of the magnitude and scale at which trees affect local air temperature in cities is hampered by the paucity of data along continuous gradients and for combinations of canopy and impervious surface.

Advances in sensor-based methods, and mobile sensors in particular, provide opportunities to quantify air temperature at data-sparse intraurban scales (21). Although stationary sensor networks are excellent for characterizing broad patterns and temporal dynamics of the UHI (22–24), mobile sensors facilitate access to areas otherwise difficult to sample and allow measurement along continuous land-cover gradients. We used a custom bicycle-based sensor (Fig. 1) to characterize intraurban heat in a midsize temperate climate city, focusing on the interaction between extent of tree canopy cover and impervious surface, but also testing for potential effects of other variables, such as relative elevation and proximity to lakes. Although others have used bicycles to study the UHI (25–27), we extend this method in multiple ways: repeated sampling of many transects on multiple days, considering continuous variation in land cover rather than assigning discrete categories, assessing effects of land cover at multiple spatial scales, and accounting for the complex spatial–temporal nature of mobile data in our statistical models. We asked, How does variability in tree canopy and impervious cover interact to influence both daytime and nighttime summer air temperature? How do these effects vary with the spatial scale at which land-cover data are analyzed? Do the effects of land cover or scales at which they matter most for air temperature change under conditions of particularly high heat?

We conducted our study in Madison, Wisconsin, a city of 255,000 people in the north central United States (28), with an urban agglomeration population of 455,000 (29). Madison is representative of many midsize cities in the Midwest and surrounding areas, and has a distinct UHI (22). Throughout summer 2016, we sampled 10 urban transects (~7 km length) at least three times each during the hottest portion of the day (e.g., ~16:00–18:00 local time), collecting data at 1-s intervals, or approximately every 5 m, given bicycle speed. We also sampled four transects at night (e.g., minimum 2 h postsunset, ~22:00–24:00 local time; Fig. 1*A*). To enable comparison of measurements collected at different times, we converted all air temperature measurements to temperature anomalies relative to fixed-reference sensors in the city center. We used generalized additive models (30) to test the effect of percentage canopy and impervious cover (Fig. 1*A*, *Inset*) and distance to the nearest of Madison's three urban lakes on summer air temperature at four scales: 10-, 30-, 60-, and 90-m radius surrounding each temperature measurement. Ranging from the approximate size of a single downtown property (10 m) to a city block (90 m), these scales are finer than typically assessed in UHI studies and are representative of the scales at which local (e.g., individual to neighborhood) actions to mitigate high air temperatures can occur.

Results

Air temperature varied substantially within the city (Fig. 1*C*). Mean within-ride daytime temperature range (i.e., difference between the hottest and coolest areas of each transect) was 3.5 °C (SE, 0.13 °C; range, 1.1–5.7 °C), whereas temperature varied by only 0.2 °C, on average, for fixed reference sensors during the same measurement periods. Variability was lower at night, with a mean within-ride temperature difference of 2.1 °C (SE, 0.13 °C; range, 1.2–3.0 °C). There was little variation in either daytime or nighttime air temperature among the 10 transects (i.e., in different geographical areas of the city), but substantial variation among individual rides on different days (i.e., driven by meteorological conditions during the sampling period; *SI Appendix*, Table S1).

Daytime Urban Heat. Air temperature decreased nonlinearly with increasing tree canopy cover (Fig. 2 *A*–*D*), and effects were larger when considered at broader compared with finer scales. Increasing canopy cover from 0% to 100% within a 10-m radius corresponded to a mean decrease of 0.7 °C in daytime air temperature (Fig. 2*A*) compared with a 1.3 °C decrease when considering a 30-m radius (Fig. 2*B*), and >1.5 °C for a 60- or 90-m radius (Fig. 2 *C* and *D*). The relationship appeared increasingly nonlinear at broader scales, particularly 60 and 90 m, with canopy cover >40% leading to substantially cooler temperatures

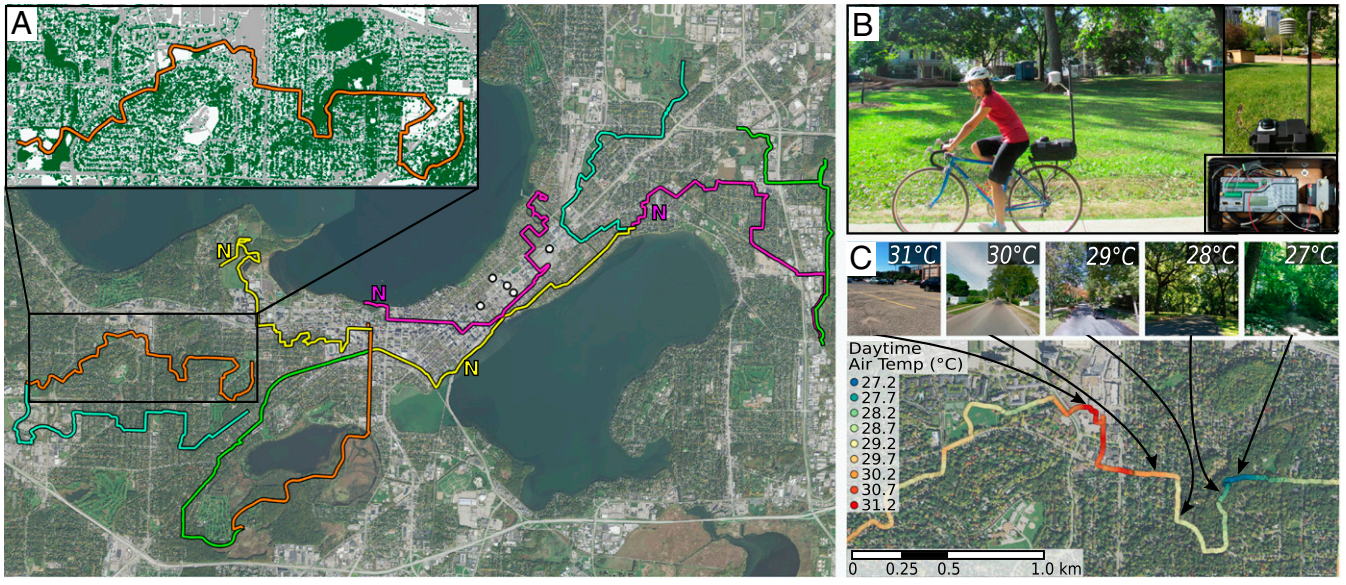

Fig. 1. A mobile sensor was used to measure variability in air temperature in Madison, Wisconsin. (*A*) Ten transects were sampled on summer days. Pink and yellow transects (marked "N") were also sampled at night. White dots represent stationary reference sensors. (*Inset*) Example of canopy and impervious cover. (*B*) Instrumentation including a fast-response, high-accuracy temperature sensor was mounted on a rear bicycle rack to facilitate continuous sampling at fine spatial scales and allow exchange among bicycles. (*C*) Raw temperature data (1 measurement/second) along a portion of one transect (same as *A*, *Inset*), demonstrating fine-scale variation in air temperature with changing land cover. Photos show land cover at various locations (indicated with arrows).

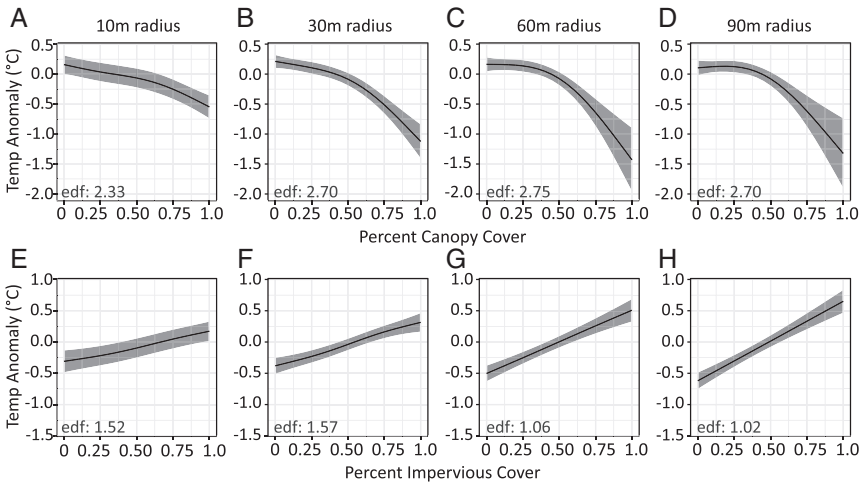

Fig. 2. Estimated smooth curves for the effect of increasing canopy cover (*A–D*) and impervious cover (*E–H*) within a surrounding radius of 10, 30, 60, and 90 m on daytime summer air temperature in Madison, Wisconsin. Black lines represent the mean, and shaded areas represent ±2 SE, both averaged across 100 models each containing 1% of the data. Mean and SEs were generated using type "iterms" in mgcv, such that SEs returned for smooth components include uncertainty about the intercept/overall mean (31). Edf represents effective degrees of freedom, averaged over all 100 models.

(Fig. 2 *C* and *D*; see *SI Appendix* for further explanation of underlying relationships).

Air temperature increased linearly with increasing impervious cover (Fig. 2). Effects were again larger when considering the surrounding landscape context at broader scales; increasing impervious cover from 0% to 100% within a 10-m radius corresponded to a mean increase of 0.5 °C (Fig. 2*E*) compared with 0.7 °C, 1.0 °C, and 1.3 °C when considering a surrounding area of radius of 30, 60, and 90 m, respectively (Fig. 2 *F–H*; see *SI Appendix* for further explanation of underlying relationships).

When jointly considering tree canopy and impervious surface cover, canopy cover reduced daytime air temperature for all amounts of impervious surface cover at all scales considered, and notably, the relative benefit of increased canopy cover in the surrounding landscape exceeded that of reducing impervious surface cover (Fig. 3). The magnitude of cooling at any given location depended on the relative amounts of canopy cover and impervious surface in the surrounding landscape (Fig. 3). For example, at the finest scale (10 m), air temperature at locations with >50% impervious surface declined by 1–1.3 °C with >75% canopy cover (Fig. 3*A*). With less impervious surface, however, the same 1 °C of cooling could be gained with only 60% canopy cover. At the largest scale (90 m), >2.5 °C of cooling could be achieved in low impervious areas with >75% canopy cover, but such strong cooling effects were unachievable with high percentage cover of impervious surfaces (Fig. 3*D*).

Interactions between canopy cover and impervious surface also became more nonlinear at larger scales (e.g., 60 and 90 m; Fig. 3 *C* and *D*). For locations with >25% impervious surface (e.g., most residential areas), air temperatures declined most rapidly when canopy cover surpassed 40%, even though absolute levels of cooling were greatest when impervious surface cover was low. For example, in a typical residential neighborhood with 30% impervious cover, increasing canopy cover from 0% to 40% within a 90-m radius would lead to a negligible change in temperature, whereas increasing canopy cover from 40% to 80% would provide a full degree of cooling (Fig. 3*D*). In an area with less impervious cover (e.g., a grassy park), increasing canopy cover within a surrounding 90-m radius from 0% to 40% would increase cooling by ∼0.3 °C, whereas increasing canopy from 40% to 80% would lead to an additional ∼0.8 °C of cooling. Note that although full canopy cover and full impervious cover often co-occur at fine spatial scales (Fig. 3*A*, black points in upper right; e.g., a paved road with a closed canopy overhead), it is difficult for high impervious and canopy cover to co-occur across larger spatial scales (Fig. 3*D*, black points absent from upper right; e.g., larger expanses of impervious cover rarely leave enough space for the tree growth required to achieve high canopy cover).

The benefit of increased tree canopy cover on daytime heat mitigation was most pronounced on the hottest days (air temperatures >30 °C). Interactions between canopy cover and impervious surfaces across scales on a hot day were similar to those for the full dataset, but mean cooling increased by 0.2–0.6 °C (cf. *SI Appendix*, Fig. S4 and Fig. 3). Thus, the benefit of growing the urban canopy may be amplified on days with more extreme heat.

Other features in the urban landscape had little influence on daytime urban air temperatures. The presence of lakes decreased adjacent temperatures by only ∼0.25 °C on average, and lake effects were largely restricted to shoreline locations. Influence declined quickly with increasing distance from the lake, with no effect remaining at distances more than ∼700 m from shore (*SI Appendix*, Fig. S5). Effects of relative elevation were unimportant for daytime air temperature in all models.

Nighttime Urban Heat. Air temperature within the city was considerably less variable at night (*SI Appendix*, Fig. S6). The effect of canopy cover was limited, with increasing canopy from 0% to 100% cover corresponding to a linear decrease of 0.3–0.5 °C (magnitude increasing with scale; *SI Appendix*, Fig. S6 *A–D*). Effects of impervious cover were as or more important than canopy cover for nighttime air temperature. Increasing impervious cover within the surrounding landscape from 0% to 100% corresponded to a linear increase of 0.3–0.7 °C (magnitude increasing with scale; *SI Appendix*, Fig. S6 *E–H*). As a consequence, variation in tree canopy and impervious surface cover led to mean nighttime temperature differences of only 0.5 °C (10 m radius) to 1.1 °C (90 m radius) across the urban landscape (30- and 60-m radius intermediate at 0.7 and 0.9 °C, respectively; *SI Appendix*, Fig. S7).

Discussion

We quantified substantial variation in summer air temperature within a temperate zone urban landscape, finding a strong influence of land-cover patterns on air temperature at different scales, and nonlinear interactions between tree canopy and impervious surface cover. Our results suggest that the most effective strategies for urban heat mitigation will involve modifications to both green and gray infrastructure. For daytime air temperature, the warming effect of impervious surfaces was effectively countered by the cooling effect of trees, especially when canopy cover was ≥40% within a radius of 60–90 m, or about the scale of a city block. Thus, urban forestry has great potential to enhance daytime temperature regulation services (13, 31), which is increasingly important in cities worldwide as climate continues to warm. However, lower cover of impervious surfaces remained critical for reducing summer air temperatures at night, given the amount of heat stored and radiated back during nighttime (4). Reduction of heat at night is particularly important from a health perspective, as high overnight temperatures contribute significantly to heat-related illness and mortality (32, 33), as the body has no opportunity to recover from daytime heat exposure.

The increased cooling effect of tree canopy cover on the hottest days, when human health (e.g., asthma sufferers) and

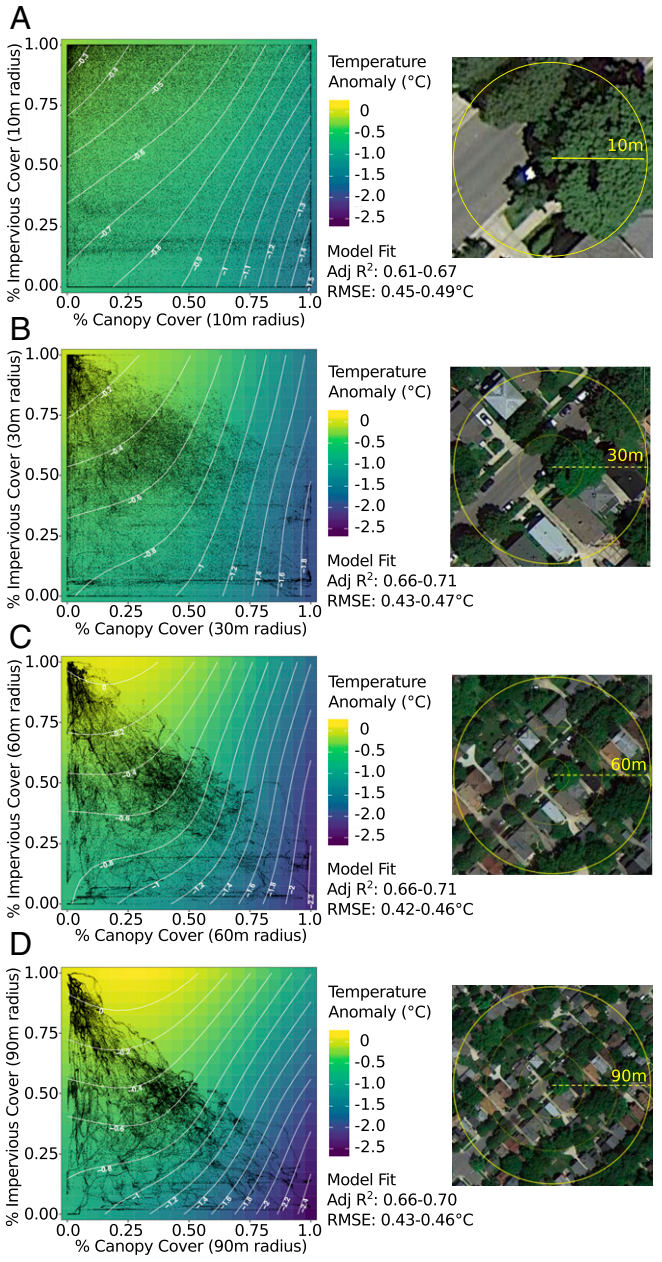

Fig. 3. Difference in daytime urban air temperature achieved through altering impervious and canopy cover within a radius of (*A*) 10 m, (*B*) 30 m, (*C*) 60 m, and (*D*) 90 m, from generalized additive model responses. Right-hand images in each panel show the scale of measurement, using an example of a medium-density neighborhood in Madison, Wisconsin. Models showed a strong relationship between observed and fitted values, with measures of model fit [adjusted R^2, root mean square error (RMSE), labeled underneath scale bar] consistent both among the 100 models at each scale and across scales.

energy impacts (e.g., air conditioning) are most consequential (5, 34–37), further underscores the importance of adaptation efforts. Our results provide insight into the likely variability of urban temperatures in a future in which such hot days will be increasingly common, and future work should more explicitly test for the interaction between meteorological conditions (including additional variables such as wind and cloud cover) and temperature regulation within cities.

The observed threshold in the effect of canopy cover on daytime air temperature has important implications for urban climate adaptation. This nonlinear relationship may also explain discrepancies in the magnitude of vegetative cooling observed in previous studies, particularly in areas with relatively low canopy cover. A stronger understanding of the underlying mechanisms of this nonlinearity is an important avenue for future research. We anticipate that this relationship is driven at least in part by the increase in leaf area index at higher levels of canopy, which increases shadows and shading. Further explanations for the nonlinearity may include an interaction between canopy cover and the nature of the surface below the canopy. Canopy cover >40% may be more likely to be shading higher amounts of impervious surface, inducing a larger cooling effect. Contrastingly, it may be that areas of high canopy cover tend to be associated with larger green spaces, and it is this combination of ground-level vegetation plus canopy that leads to increased cooling. Further research is warranted to test these hypotheses explicitly.

Although the literature on urban heat focuses predominantly on urban–rural differences, our results clearly demonstrated that the magnitude of variation in air temperature within cities can be as large as that associated with the UHI. The variation we detected in daytime air temperature within the city of Madison was comparable in magnitude to the temperature difference between the city's urban core and the surrounding rural landscape (22). That temperature variation within the city was greatest during high-heat events is also consistent with the overall UHI, which is stronger during heat waves (38). However, in contrast to the strong nighttime urban–rural differences in Madison (22) and elsewhere (4), nighttime temperature differences within the city were diminished (6). Canopy provides cooling through both shading (blocking incoming thermal radiation and preventing impervious surfaces from absorbing and reradiating it) and evapotranspiration. The reduced effect of canopy at night is likely in part because of the lack of evapotranspirative cooling once photosynthesis shuts down. This effect may also be explained in part by the aggregate effects of heat stored in impervious surfaces across the urban landscape, with nighttime radiation potentially trapped within the city by built infrastructure (especially narrow "urban canyons"), and even urban tree canopy. These differences in daytime and nighttime results highlight the importance of an improved understanding of fine-scale drivers of urban heat, and also suggest that high daytime temperatures may be more easily managed via land-cover modifications (e.g., increased tree cover) than nighttime temperatures. Thus, although our results provide guidance regarding priorities for tree planting to reduce daytime temperatures, we advocate for reducing impervious surfaces as a component of any urban climate adaptation plan.

The mitigation potential of land-cover patterns within cities gives urban stakeholders at various levels of governance (e.g., residents, property managers, urban planners) agency over reducing daytime summer temperatures. Where to allocate limited tree planting resources will depend on many factors in addition to temperature regulation. However, results of this study can be used to identify areas in which planting new trees may most effectively mitigate urban heat.

Where Should Trees Be Planted to Cool the City Most Effectively? Canopy cover in excess of ∼40% had a larger effect on temperature reduction. Furthermore, temperature differences were strongest, and increasing canopy had the greatest effect, at scales of ∼60–90 m (comparable in Madison to the area of a typical city block). Thus, neighborhoods with intermediate amounts of impervious surface and ≥40% canopy cover could offer the greatest marginal increase in climate mitigation for urban residents. High canopy neighborhoods where significant future canopy loss is anticipated, for example because of invasive insects such as emerald ash borer (*Agrilus planipennis*, ref. 39) or an aging tree population, would also be priority areas. At this neighborhood scale, significant increases in (or maintenance of) canopy will require multistakeholder collaboration; a persistent challenge of urban ecology (40). For example, trees planted along streets, on private property, and in public parks may have to be strategically

located to increase canopy cover above a threshold to induce a meaningful reduction in summer temperatures.

Although prioritizing areas ≥40% canopy may increase cooling the most, it is important to ensure that planting efforts do not occur exclusively in areas in which tree cover is already high. Climate adaptation efforts must also consider the social and environmental (in)justice issues embedded within many cities. A history of class and racial inequality and oppression has led to considerable inequalities in access to green space and environmental amenities in contemporary cities (41, 42). Tree cover is often highest in wealthy, predominantly white areas (43), whereas densely built-up areas, and those with the lowest vegetation cover, are often home to populations for which access to resources to combat increased heat (e.g., air conditioning) is lacking (44, 45). Societal vulnerability to extreme heat must be considered alongside landscape context in any planning initiative.

When Does Local Planting Matter? The cooling effect of canopy is weaker at fine scales than broader, as a very small area of canopy cannot be isolated from the surrounding meteorological conditions (further explanation in *SI Appendix*). Analogously, the ocean exerts a stronger influence on the weather at the center of a 10-km-wide island compared with an island 100 km wide. Nevertheless, increasing tree canopy cover within only a 10–30-m radius [an area comparable in Madison to a single downtown lot (10 m) or two to three suburban properties (30 m)] still yielded measurable cooling. Thus, there is a role for planting trees in targeted locations where people will benefit directly; for example, adjacent to a house or yard, or along a well-used walking path. However, these planting decisions should recognize that benefits may be small if the surrounding area is low canopy.

The strong and nonlinear effect of tree canopy also suggests balance is needed in urban planning and design between the compact urbanization suggested for maintaining many ecosystem services and a somewhat less dense urbanization in which built and natural spaces are interspersed (46). More compact urban building footprints likely limit the ability of a tree canopy to flourish, given limited space and access to soils in the densest urban areas (explaining the lack of empirical data in the "high-canopy, high impervious" category at larger scales), requiring innovative planning and design solutions. Although it is important to be cognizant of the negative ecological effects of urban sprawl (46, 47), combatting urban heat where people live also requires incorporation of enough green space within our cities to achieve effective levels of canopy cover, which may be particularly difficult in higher-density neighborhoods or areas subject to in-filling.

Because of the long-lived nature of trees and persistence of pavement, current decisions (from homeowner preferences to urban planning choices and urban forest policy) are setting up the urban heat riskscape of the future (19). Thoughtful choices today are needed to ensure the resilience of our future cities, and will rely at least in part on city programs, homeowner education, or other incentives. Further studies of urban air temperature at fine-scales within cities are also needed to confirm the generality of our findings, and further clarify underlying mechanisms. Our methods provide guidance for affordable, low-impact measurement of the intraurban heat island, and could be replicated to test mitigation strategies in cities that vary in urban form, population, or geographic region. Methods may also be amenable to citizen science sampling programs, offering a mechanism to further engage urban populations in the development of climate adaptation measures that will be critical as our cities warm.

Methods

Study Area. Madison, Wisconsin, is a midsize city centered on two lakes in the north-central United States (43.0731° N, 89.4012° W). The climate is humid-continental, with warm humid summers and cold winters [1981–2010 mean temperature, 22 °C July, −7 °C January; annual precipitation, 87.6 cm (48)]. Characterized predominantly by low-density housing, Madison also contains mid- and high-density development, as well as green spaces including forest, wetland, and prairie (49). The surrounding landscape is largely agricultural, but includes remnant native vegetation (forests and grasslands), wetlands, and several lakes (50).

Mobile Measurements. We built two bicycle-mounted temperature sensors (Fig. 1*B*) equipped with instrumentation to quantify human thermal exposure. A fast-response, high-accuracy temperature probe (Campbell Scientific 109SS) equipped with solar shield was mounted at 1.5 m high, with a response time of <7.5 s in 3 m/s wind and an accuracy of ±0.1 °C. This sensor and a GPS device (Campbell Scientific GPS16X-HVX) were integrated directly with a data logger (Campbell Scientific CR-850) and sealed lead acid rechargeable battery, enabling simultaneous recording of temperature and location while riding.

Ten urban transects were selected to cover the city geographically (Fig. 1*A*) and span a wide range of variability in canopy and impervious cover. Mean transect length was 7 km (mean cycling time, 28 min) to avoid large changes in background temperature during measurement periods. During summer 2016 (May 30–September 6), each transect was sampled at least three (but up to 12) times during the hottest portion of the day (always between 1:30 and 7 PM, but usually between 4 and 6 PM), for 64 total daytime rides. Four transects (Fig. 1*A*) were also sampled at night (minimum 2 h after sunset, ∼10 PM–12 AM), for 12 total rides at night. Maximum daily temperature averaged 29 °C on sampling days (range, 22–34 °C). Other meteorological conditions varied across sampling periods (mean wind speed, 12.5 km·h^{-1}, ranging from calm to 35 km·h^{-1}; mean relative humidity, 58%, ranging from 35% to 94%; cloud cover, ranging from clear to overcast, with a mix of sun and cloud most common), with night conditions typically more humid and less windy.

Data were collected at 1-s intervals, corresponding to air temperature observations approximately every 5 m. Repeated measurements at any particular location (e.g., while at a stoplight) were removed to avoid potential measurement errors; for example, because of exhaust or engine heat from surrounding cars. To facilitate comparison of measurements collected at different times, measurements were converted to temperature anomalies, using the mean temperature at a given time of five stationary sensors in the city center, where temperatures are typically warmest, as a reference data set (Fig. 1*A*; see *SI Appendix* for more detail). Thus, a temperature anomaly of −1 °C corresponds to temperature at the measurement location 1 °C lower than the average temperature of the reference sensors at the same time.

Landscape Structure. We calculated percentage canopy and impervious cover (Fig. 1*A*, *Inset*) within a series of buffers (of 10-, 30-, 60-, and 90-m radius) surrounding each temperature measurement. Canopy cover was calculated from a 1-m-resolution urban land-cover raster derived from National Agriculture Imagery Program data. Impervious cover was calculated from a custom layer composed of (LiDAR-derived) building footprints and City of Madison open data for stormwater impervious areas, roads, and bicycle paths (https://data-cityofmadison.opendata.arcgis.com). This layer was hand-corrected by referencing high-resolution satellite imagery and rasterized at 1-m resolution. For each measurement, we also calculated distance to water and relative elevation (relative to mean elevation of the corresponding transect; from National Elevation Dataset 10 m digital elevation model). Analysis was performed using QGIS.

Data Analysis. To evaluate the effects of canopy and impervious cover on summer air temperatures at each scale of interest, we used generalized additive models (GAMs, using the "bam" function in R package "mgcv" version 1.8.17; 30). GAMs are a flexible, nonparametric technique that use penalized regression splines to fit smooth relationships between response and explanatory variables. We assumed temperature was normally (Gaussian) distributed.

Percentage impervious cover, canopy cover, and their interaction were included as smooth terms, as was distance from water. Smooths for single variables were fit using thin plate splines with a null space penalty (30). The interaction term was fit using a tensor product interaction (ti) term. We restricted the maximum degrees of freedom below mgcv defaults (allowing three basis functions per smooth term and nine for the interaction) to account for the fact that GAMs can overestimate nonlinearity of functional relationships in the presence of strong spatial autocorrelation (30). Spatial coordinates were also included as a smooth term to account for unspecified spatial structure beyond that explained by land-cover variables. This term was fit using a Gaussian process spline with the default Matern covariance function (51), using 29 basis functions to allow considerable flexibility in the shape of this relationship. Elevation was not a significant driver of temperature in our low topographic-relief system, and was excluded from final models. For all models, rides were nested within transect as a random effect (intercept) to account for differences in underlying weather conditions during different sampling periods. Models were fit using fast restricted maximum likelihood (52).

Because of measurement frequency, considerable temporal autocorrelation was present in model residuals when the GAM model was fit using the entire data set. To account for the fact that positive spatial or temporal autocorrelation reduces effective sample size (53), data were partitioned into 100 subsets of 1% of the data, each composed of measurements equally spaced in time (e.g., model one included measurements 1, 101, 201...; model two included measurements 2, 102, 202...). We averaged the predictions from each model to determine the response of temperature to explanatory variables (Fig. 2). Including only every 100th point in each model considerably reduced residual autocorrelation (based on assessment of pacf plots), whereas averaging responses across 100 models ensured full use of available information, and incorporated intermodel variation in our estimate of uncertainty in the shape of functional responses.

We repeated this approach for the hottest days (where mean temperature for 4 h before sampling exceeded 30 °C) to determine whether UHI effects were exacerbated under high heat conditions. We also repeated our approach with nighttime measurements (excluding distance from water, as the effect was not significant at night).

Data and Code Availability. All data and code are available through the Environmental Data Initiative (54).

ACKNOWLEDGMENTS. We thank C. Gratton, E. Damschen, S. Carpenter, and J. Schatz for helpful comments on the development of these ideas. We appreciate logistical support from University of Wisconsin–Madison Instrument Maker Joel Lord, field assistance from Chloe Wardropper and Olivia Cope, and access to detailed canopy data from Tedward Erker. We acknowledge funding from the US National Science Foundation, especially the Long-Term Ecological Research (DEB-1440297) and Water Sustainability and Climate (DEB-1038759) Programs, and support to M.G.T. from the University of Wisconsin-Madison Vilas Trust. C.D.Z. acknowledges support from a Natural Science and Engineering Research Council of Canada doctoral fellowship, and Garden Club of America Zone VI Fellowship in Urban Forestry.

1. Oke TR (1982) The energetic basis of the urban heat island. *Q J R Meteorol Soc* 108:1–24.
2. Arnfield AJ (2003) Two decades of urban climate research: A review of turbulence, exchanges of energy and water, and the urban heat island. *Int J Climatol* 23:1–26.
3. Patz JA, Campbell-Lendrum D, Holloway T, Foley JA (2005) Impact of regional climate change on human health. *Nature* 438:310–317.
4. Memon RA, Leung DYC, Chunho L (2008) A review on the generation, determination and mitigation of urban heat island. *J Environ Sci (China)* 20:120–128.
5. Tan J, et al. (2010) The urban heat island and its impact on heat waves and human health in Shanghai. *Int J Biometeorol* 54:75–84.
6. Jenerette GD, et al. (2016) Micro-scale urban surface temperatures are related to land-cover features and residential heat related health impacts in Phoenix, AZ USA. *Landsc Ecol* 31:745–760.
7. The Weather Channel (2018) All-time heat records set worldwide since late June. Available at https://weather.com/news/weather/news/2018-07-05-all-time-temperature-record-set-worldwide. Accessed October 20, 2018.
8. Seto KC, Golden JS, Alberti M, Turner BL, 2nd (2017) Sustainability in an urbanizing planet. *Proc Natl Acad Sci USA* 114:8935–8938.
9. Mishra V, Ganguly AR, Nijssen B, Lettenmaier DP (2015) Changes in observed climate extremes in global urban areas. *Environ Res Lett* 10:024005.
10. Buyantuyev A, Wu J (2009) Urban heat islands and landscape heterogeneity: Linking spatiotemporal variations in surface temperatures to land-cover and socioeconomic patterns. *Landsc Ecol* 25:17–33.
11. White-Newsome JL, et al. (2013) Validating satellite-derived land surface temperature with in situ measurements: A public health perspective. *Environ Health Perspect* 121:925–931.
12. Bowler DE, Buyung-Ali L, Knight TM, Pullin AS (2010) Urban greening to cool towns and cities: A systematic review of the empirical evidence. *Landsc Urban Plan* 97:147–155.
13. Hiemstra JA, Saaroni H, Amorim JH (2017) The urban heat Island: Thermal comfort and the role of urban greening. *Future City* (Springer International Publishing, Cham, Switzerland).
14. Cadenasso ML, Pickett ST, Schwarz K (2007) Spatial heterogeneity in urban ecosystems: Reconceptualizing land cover and a framework for classification. *Front Ecol Environ* 5:80–88.
15. Zhou W, Pickett STA, Cadenasso ML (2017) Shifting concepts of urban spatial heterogeneity and their implications for sustainability. *Landsc Ecol* 32:15–30.
16. Conway TM (2016) Tending their urban forest: Residents' motivations for tree planting and removal. *Urban For Urban Green* 17:23–32.
17. Pickett STA, et al. (2017) Dynamic heterogeneity: A framework to promote ecological integration and hypothesis generation in urban systems. *Urban Ecosyst* 20:1–14.
18. Roman LA, et al. (2018) Human and biophysical legacies shape contemporary urban forests: A literature synthesis. *Urban For Urban Green* 31:157–168.
19. Gago EJ, Roldan J, Pacheco-Torres R, Ordóñez J (2013) The city and urban heat islands: A review of strategies to mitigate adverse effects. *Renew Sustain Energy* 25:749–758.
20. Gage EA, Cooper DJ (2017) Relationships between landscape pattern metrics, vertical structure and surface urban heat island formation in a Colorado suburb. *Urban Ecosyst* 20:1229–1238.
21. Advisory Committee for Environmental Research and Education (2018) Sustainable urban systems: Articulating a long-term convergence research agenda. A report from the NSF Advisory Committee for Environmental Research and Education (Prepared by the Sustainable Urban Systems Subcommittee). Available at https://www.nsf.gov/ere/ereweb/ac-ere/sustainable-urban-systems.pdf. Accessed October 20, 2018.
22. Schatz J, Kucharik CJ (2014) Seasonality of the urban heat island effect in Madison, Wisconsin. *J Appl Meteorol Climatol* 53:2371–2386.
23. Smoliak BV, Snyder PK, Twine TE, Mykelby PM, Hertel AWF (2015) Dense network observations of the twin cities canopy-layer urban heat island. *J Appl Meteorol Climatol* 54:1899–1917.
24. Chen Y-C, Yao C-K, Honjo T, Lin T-P (2018) The application of a high-density street-level air temperature observation network (HiSAN): Dynamic variation characteristics of urban heat island in Tainan, Taiwan. *Sci Total Environ* 626:555–566.
25. Brandsma T, Wolters D (2012) Measurement and statistical modeling of the urban heat island of the city of Utrecht (The Netherlands). *J Appl Meteorol Climatol* 51: 1046–1060.
26. Heusinkveld BG, et al. (2014) Spatial variability of the Rotterdam urban heat island as influenced by urban land use. *J Geophys Res Atmos* 119:677–692.
27. Rajkovich NB, Larsen L (2016) A bicycle-based field measurement system for the study of thermal exposure in Cuyahoga County, Ohio, USA. *Int J Environ Res Public Health* 13:159.
28. US Bureau (2010) State and county quick facts. Available at www.census.gov/quickfacts. Accessed October 20, 2018.
29. Demographia (2018) Demographia world urban areas (urban agglomerations). 14th Annual Edition. Available at www.demographia.com/db-worldua.pdf. Accessed October 20, 2018.
30. Wood SN (2017) *Generalized Additive Models: An Introduction with R* (CRC Press, Boco Raton, FL), 2nd Ed.
31. Adams MP, Smith PL (2014) A systematic approach to model the influence of the type and density of vegetation cover on urban heat using remote sensing. *Landsc Urban Plan* 132:47–54.
32. Laaidi K, et al. (2012) The impact of heat islands on mortality in Paris during the August 2003 heat wave. *Environ Health Perspect* 120:254–259.
33. McGeehin MA, Mirabelli M (2001) The potential impacts of climate variability and change on temperature-related morbidity and mortality in the United States. *Environ Health Perspect* 109:185–189.
34. Basu R (2009) High ambient temperature and mortality: A review of epidemiologic studies from 2001 to 2008. *Environ Health* 8:40.
35. Abel DW, et al. (2018) Air-quality-related health impacts from climate change and from adaptation of cooling demand for buildings in the eastern United States: An interdisciplinary modeling study. *PLoS Med* 15:e1002599.
36. Li D, Bou-Zeid E (2013) Synergistic interactions between urban heat islands and heat waves: The impact in cities is larger than the sum of its parts. *J Appl Meteorol Climatol* 52:2051–2064.
37. Anderson GB, Bell ML (2011) Heat waves in the United States: Mortality risk during heat waves and effect modification by heat wave characteristics in 43 U.S. communities. *Environ Health Perspect* 119:210–218.
38. Schatz J, Kucharik CJ (2015) Urban climate effects on extreme temperatures in Madison, Wisconsin, USA. *Environ Res Lett* 10:1–13.
39. Poland TM, Forestry DMJO (2006) Emerald ash borer: Invasion of the urban forest and the threat to North America's ash resource. *J For* 104:118–124.
40. Aronson MF, et al. (2017) Biodiversity in the city: Key challenges for urban green space management. *Front Ecol Environ* 15:189–196.
41. Grove M, et al. (2017) The legacy effect: Understanding how segregation and environmental injustice unfold over time in Baltimore. *Ann Am Assoc Geogr* 108:524–537.
42. Hope D, et al. (2003) Socioeconomics drive urban plant diversity. *Proc Natl Acad Sci USA* 100:8788–8792.
43. Schwarz K, et al. (2015) Trees grow on money: Urban tree canopy cover and environmental justice. *PLoS One* 10:e0122051.
44. Harlan SL, et al. (2008) In the shade of affluence: The inequitable distribution of the urban heat island. *Res Soc Probl Public Policy* 15:173–202.
45. Jenerette GD, Harlan SL, Stefanov WL, Martin CA (2011) Ecosystem services and urban heat riskscape moderation: Water, green spaces, and social inequality in Phoenix, USA. *Ecol Appl* 21:2637–2651.
46. Stott I, Soga M, Inger R, Gaston KJ (2015) Land sparing is crucial for urban ecosystem services. *Front Ecol Environ* 13:387–393.
47. Geschke A, James S, Bennett AF, Nimmo DG (2018) Compact cities or sprawling suburbs? Optimising the distribution of people in cities to maximise species diversity. *J Appl Ecol* 55:2320–2331.
48. National Climatic Data Center (2018) Data tools: 1981-2010 normals. Available at www.ncdc.noaa.gov/cdo-web/datatools/normals. Accessed October 20, 2018.
49. Ziter C, Turner MG (2018) Current and historical land use influence soil-based ecosystem services in an urban landscape. *Ecol Appl* 28:643–654.
50. Carpenter SR, et al. (2007) Understanding regional change: Comparison of two lake districts. *Bioscience* 57:323–335.
51. Kammann EE, Wand MP (2003) Geoadditive models. *J R Stat Soc Ser C Appl Stat* 52:1–18.
52. Wood SN, Goude Y, Shaw S (2015) Generalized additive models for large data sets. *J R Stat Soc Ser C Appl Stat* 64:139–155.
53. Fortin MJ, Dale MRT (2005) *Spatial Analysis: A Guide for Ecologists* (Cambridge Univ Press, Cambridge, UK).
54. Ziter CD, Pedersen DJ, Kucharik CJ, Turner MG (2019) Data from: "Scale-dependent interactions between tree canopy cover and impervious surfaces reduce daytime urban heat during summer." Environmental Data Initiative. Available at https://portal.edirepository.org/nis/mapbrowse?packageid=edi.314.2. Deposited February 12, 2019.